Feedback control stabilizing the center of mass can be identified in unperturbed, upright standing

Yang Geng[a], Sjoerd M. Bruijn[a], Jaap H. van Dieën [a]*

[a] *Department of Human Movement Sciences, Faculty of Behavioral and Movement Sciences, Amsterdam Movement Sciences, Vrije Universiteit Amsterdam, Amsterdam, The Netherlands*

* Corresponding author at: Van der Boechorststraat 9, 1081 BT Amsterdam, the Netherlands.
E-mail address: j.van.dieen@vu.nl (Jaap H. van Dieën).

Abstract

Feedback stabilization of upright standing should be reflected by a time-lagged relationship between the ground reaction force (GRF) and the center of mass (COM) state. In this study, we propose a model relating corrective ground reaction forces (F_{corr}) to preceding COM position (PCOM) and velocity (VCOM). We first checked the model's validity by simulating an inverted pendulum model with known intrinsic and feedback parameters, to see whether and to what extend we could effectively identify the feedback parameters. Next, we tested the model in 15 young adult volunteers in standing.

Our model effectively reconstructed F_{corr} in both simulations (R^2: 0.77~0.99) and human experimental data (R^2: 0.92~0.98). The effective delay in the mediolateral direction (239 ± 20 ms) was significantly shorter than in the anteroposterior direction (271 ± 28 ms). Additionally, position gains were significantly larger in the mediolateral compared to anteroposterior direction, with values of -1.09 ± 0.04 and -1.03 ± 0.02 times critical stiffness, respectively. No significant differences between the directions were found in velocity gains.

Our model can be used to identify feedback control in human standing without applying external perturbations or measuring physiology activity. Although the estimated parameters represent the lumped effects of both intrinsic and feedback contributions, they remain informative of the feedback mechanism because the intrinsic impact is negligible under normal standing. Our results show that stability of upright stance in healthy young adults is achieved by position feedback gains at levels just above critical stability. The proposed model requires easily measurable inputs which may yield value in assessment of balance disorders.

1. Introduction

Even when we are 'standing still', our bodies are never completely static and display subtle sway. Without any appropriate corrections to naturally occurring internal perturbations and various external disturbances, we will lose stability and encounter a subsequent fall. Stabilization of upright standing can be simplified as the control of the body's COM relative to its base of support, which can be achieved by feedback control based on COM position and velocity (Pai & Patton, 1997).

Different measures reflecting control actions to stabilize the body have been used to investigate feedback control in standing. Measures such as electromyography (EMG) and ankle torque show a time-lagged relationship with the COM state after perturbations. For example, a linear feedback model with delayed COM deviations as input explained more than 47% and 60% variance in dominate reactive muscle activities following discrete and continuous perturbations, respectively (Safavynia & Ting, 2013) and up to 94% of the variance in reactive ankle moments (Afschrift, De Groote, & Jonkers, 2021) in perturbed standing. Although these models are highly effective and provide valuable insights into feedback control mechanisms, they require complex measurements and external perturbations. Here, we asked whether a simple model, which requires only easily obtainable variables and an estimate of the center of mass, can be used to estimate feedback control parameters.

Any corrective actions to remain stable while standing should ultimately be reflected in the ground reaction forces. Indeed, it has been shown that the horizontal ground reaction forces during standing contain meaningful information about neural control strategies (Shiozawa, Lee, Russo, Sternad, & Hogan, 2021; Sugimoto-Dimitrova, Shiozawa, Gruben, & Hogan, 2024). Therefore, we hypothesize that stability control in standing can be represented by a linear relationship between the corrective ground reaction force and the delayed COM state. Such a relationship has recently been modeled in a study on unperturbed walking (van Dieen, Bruijn, & Afschrift, 2024). In this study, the COM state during unperturbed walking was shown to predict the ground reaction force after some delay. This suggests that (at least during walking) not only during or shortly after perturbations, delayed feedback control based on COM information is used. If a similar model can be used to characterize control of standing, it can be estimated from easily obtainable data measured during unperturbed standing: COM position and velocity on one the hand, and horizontal ground reaction forces or COM acceleration on the other hand.

However, it is obvious that humans do not only use feedback control to stabilize standing posture, as passive mechanisms (i.e., intrinsic stiffness, damping, inertia) also play a role (Amiri, Mohebbi, & Kearney, 2019; Peterka, 2002). Muscles provide short-range intrinsic stiffness, which will generate instantaneous torque to resists movement

prior to any involvement of the nervous system (De Groote, Allen, & Ting, 2017). In addition, muscle's length-velocity-force relationship provides effects which can be modeled as stiffness and damping (de Vlugt et al., 2011; Latash & Zatsiorsky, 1993; Rack & Westbury, 1974). The impedance determined by the intrinsic properties of muscles acts in parallel with active feedback control, which may make estimating the feedback component hard, especially in natural standing without any perturbations. Moreover, human stability control may be intermittent, with a "switch-like" controller, where feedback is only present when the body sways beyond a certain area (dead zone) (De Groote et al., 2017; Kelton & Wright, 1949; Loram, Gollee, van de Kamp, & Gawthrop, 2022; Milton, Townsend, King, & Ohira, 2009). Such intermittent characteristics potentially cause additional challenges when trying to estimate feedback control parameters from unperturbed human standing.

We here propose to use a simplified feedback model to estimate the feedback parameters from unperturbed standing, in spite of the possible intermittent characteristic of human stability control, and the presence of intrinsic stiffness and damping. van der Kooij, van Asseldonk, and van der Helm (2005) have argued that feedback and intrinsic contributions to stabilization cannot be distinguished without applying known external perturbations. Here, we assessed whether applying perturbations can be avoided by fitting a model reflecting the lumped effects of both intrinsic and feedback. Then, we asked if, and to what extent the estimated lumped parameters are still informative about feedback control. Our simulation results show that corrective ground reaction forces can be well reconstructed from the preceding COM state in these simulations, and the estimated feedback parameters were correlated to the actual feedback parameters, which indicates that this method may be applicable to investigate feedback control in humans. Then, we applied the model to experimental data from human volunteers to assess feedback control of standing in humans. By analyzing the estimated feedback gains and delays, we can obtain valuable insights into how the central nervous system controls stability under normal conditions. Moreover, our model could serve as a useful framework for assessing balance disorders.

2. Methods

2.1. Model simulation

In this study, we modelled the human body as an inverted pendulum (IP) oscillating around the ankle(Gage, Winter, Frank, & Adkin, 2004; Gatev, Thomas, Kepple, & Hallett, 1999; Winter, Patla, Prince, Ishac, & Gielo-Perczak, 1998), controlled by intrinsic and feedback properties, as illustrated in Figure 1 and equation (1). We here focus on controlling the IP model sway in the anteroposterior (AP) direction, while the model is equally applicable to the mediolateral (ML) direction based on the fact that the upper and lower body motion move in-phase at low frequencies in both the sagittal (Creath, Kiemel, Horak, Peterka, & Jeka, 2005) and frontal plane (Goodworth & Peterka, 2010).

The feedback mechanism generates a feedback moment (M_{fd}), which is angle (θ) and angular velocity ($\dot{\theta}$) dependent, with a delay (τ). Both for the angle and angular velocity, we defined a dead zone ($\theta_d,\ \dot{\theta}_d$) acting as a switch on feedback control. When the body sways within these thresholds, no feedback will be provided, while when either of these thresholds is exceeded, position- and/or velocity-dependent feedback will be provided. In effect, the system becomes intermittently controlled.

For the intrinsic and feedback control parameters, previous studies have reported a wide range of values. For example, estimates of intrinsic stiffness ranged from relatively low (0.7~2.3 Nm/deg) as reported by Peterka (2002), to substantially higher (10~12 Nm/deg) as reported by Loram and Lakie (2002). Similarly, reported intrinsic damping varies widely, from lower than 0.1 Nms/deg (Loram & Lakie, 2002; Ribeiro, Knop, & Rastgaar, 2020), to much higher values of 1.8~2.2 Nms/deg (Sakanaka, Gill, Lakie, & Reynolds, 2018). Feedback position gain has been reported within a range of 10~20 Nm/deg, while feedback velocity gain has been found to vary from 3.5 to 7 Nms/deg in free standing (Peterka, 2002). In our study, the initial parameters were set to the mean values reported by Peterka (2002), as this allows us to use both feedback and intrinsic parameter estimates from one single study.

The default feedback delay was set at 150ms, consistent with 150~200ms delays reported in previous studies (Casadio, Morasso, & Sanguineti, 2005; Peterka, 2002). The position dead zone was set as 0.23 deg, matching the values used by Asai et al. (2009), and the velocity dead zone was accordingly set at 0.092π deg/s based on the physical relationship between position and velocity assuming a dominant sway frequency of 0.2 Hz (Peterka, 2002). To incorporate motor noise, we injected low-pass filtered (5 Hz) (Mello, Magalhaes, & Kohn, 2013) random noise with an amplitude of 0.2 Nm based on Shi, Rymer, and Son (2023). Sensory position noise was set as 0.3 Nm/deg to achieve realistic sway, and sensory velocity noise was accordingly set as 0.377 Nms/deg. Table 1 presents the default parameters of the model.

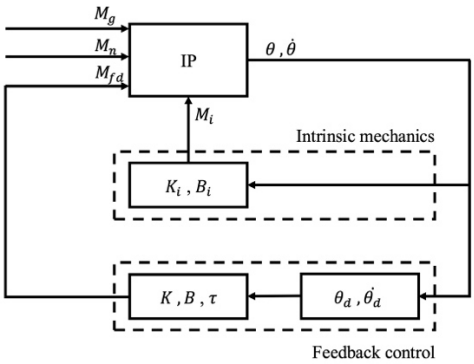

Figure 1. Inverted pendulum model with feedback. IP represents the inverted pendulum with continuously changing angular (θ) and angular velocity ($\dot{\theta}$) as the system's states. The intrinsic mechanics generates an intrinsic moment (M_i) based on the current θ and $\dot{\theta}$ and the intrinsic stiffness (K_i) and damping (B_i). In the feedback mechanism, $\theta_d,\ \dot{\theta}_d$

represent the dead zone for angular and angular velocity respectively, acting as switches determining whether feedback control is activated. When a "switch" turns on, the feedback mechanism generates a moment (M_{fd}) based on the time-lagged IP state with feedback position gain (K) and feedback velocity gain (B) and time delay (τ). M_n and M_g represent moments generated by sensorimotor noise and gravity, respectively.

Mathematically our model takes the form of:

$$I * \ddot{\theta}_i = M_{g_i} + M_{n_i} + \left(K_i * \theta_i + B_i * \dot{\theta}_i\right) + \left(K * \theta_{i-\tau} * H\left(|\theta_{i-\tau}| > \theta_{d_{i-\tau}}\right) + (B * \dot{\theta}_{i-\tau} * H\left(\left|\dot{\theta}_{i-\tau}\right| > \dot{\theta}_{d_{i-\tau}}\right)\right) \quad (1)$$

where I represents the inertia, approximated by modeling the human body as a cylinder, which can be calculated by $1/12 * m * (3 * {r_{IP}}^2 + h^2) + m * l^2$, where m is the body mass, r_{IP} is the radius of cylinder, h is the body height, and l is the IP length/COM height. $\ddot{\theta}$ is the angular acceleration. M_g and M_n represent the gravitational and sensorimotor noise moment, K_i and B_i are the intrinsic stiffness and damping, θ and $\dot{\theta}$ represent the angle and angular velocity, i represents the current time. H is the Heaviside function with θ_d, $\dot{\theta_d}$ the magnitude of the dead zones. The third term $\left(K_i * \theta_i + B_i * \dot{\theta}_i\right)$ represents the moment generated by intrinsic mechanics without time delay. The last term $\left(K * \theta_{i-\tau} \times H\left(|\theta_{i-\tau}| > \theta_{d_{i-\tau}}\right) + (B * \dot{\theta}_{i-\tau} \times H\left(\left|\dot{\theta}_{i-\tau}\right| > \dot{\theta}_{d_{i-\tau}}\right)\right)$ is the moment generated by time-lagged feedback control , with K and B as the feedback position and velocity gains and τ representing the delay.

Table 1. IP simulation parameters. Note that the velocity dead zone ($\dot{\theta_d}$) and sensory velocity noise (N_{s1}) were derived from positional parameters and varied synchronously with their corresponding position parameters across simulations.

Parameters	Default value	Variations	Unit
body mass (m)	80	-	kg
body height (h)	1.8	-	m
IP length (l)	0.9	-	m
radius (r_{IP})	0.14	-	m
gravity acceleration (g)	9.81	-	m/s^2
intrinsic stiffness (K_i)	1.6	40%, 100%, 600%	Nm/deg
intrinsic damping (B_i)	0.43	50%, 100%, 500%	Nms/deg
feedback position gain (K)	16.9	60%, 100%, 120%	Nm/deg
feedback velocity gain (B)	5.8	60%, 100%, 110%	Nms/deg
position dead zone (θ_d)	0.23	0, 100%	deg
velocity dead zone ($\dot{\theta_d}$)	0.29	0, 100%	deg/s
motor noise (N_m)	0.2	50%, 100%, 200%	Nm
sensory position noise (N_{s0})	0.3	50%, 100%, 120%	Nm/deg
sensory velocity noise (N_{s1})	0.377	50%, 100%, 120%	Nms/deg
feedback delay (τ)	150	70%, 100%, 130%	ms

First, we validated our model by performing 10 repetitions using the default parameters, without incorporating dead zones or intermittency. Then we performed a systematic variation of these parameters to comprehensively understand how model parameters would influence the estimated feedback parameters. Specifically, the feedback parameters were constrained within the ranges reported by Peterka (2002). For intrinsic parameters, we adjusted them to cover the range of estimates in different studies. Each parameter was varied across the levels as specified in Table 1, and all parameters were combined using a full factorial design, except that the velocity dead zone and sensory velocity noise were not changed independently. Instead, these two velocity-related parameters were mathematically derived from their positional parameters, generating in total 4374 unique parameter combinations. For each combination, we simulated the model for 60s and repeated 10 times to ensure statistical reliability. Some parameter combinations produced unrealistic sway and even instability, we therefore excluded simulations with sway amplitude exceeding 0.1 rad (the maximum mean sway (5.58 deg) reported by Winter, Patla, Rietdyk, and Ishac (2001)), resulting in 3328 valid parameter combinations. These unrealistic combinations were also analyzed to better understand which parameters/combinations led to instability (see Table 3).

Based on equation (1), we obtained the total moment exerted on the IP model, from which we calculated angular acceleration ($\ddot{\theta}$). Then we used simple Euler integration, with integration steps of 2ms to obtain the angular velocity ($\dot{\theta}$) and angle (θ). Using the simulated data, we further calculated the kinematics of the IP center of mass (i.e., position (PCOM), velocity (VCOM), and acceleration (aCOM)) and the ground reaction force in AP direction (F_{AP}) by Newton's second law.

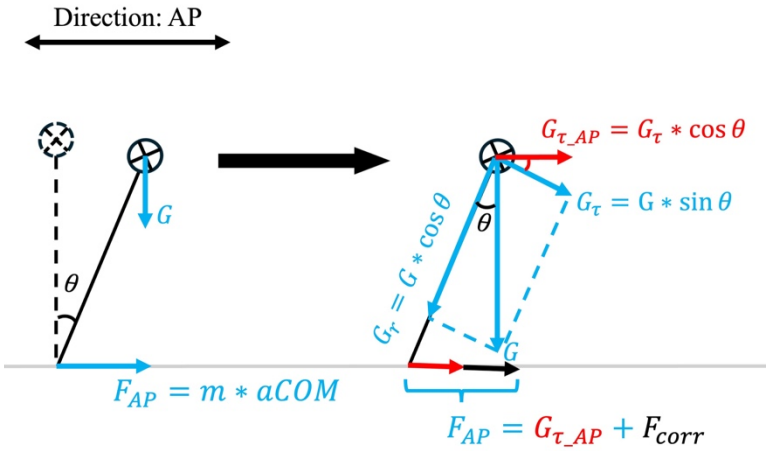

Figure 2. Calculation of corrective ground reaction force. The left plot represents the IP state, with the dashed line indicating a perfectly upright state perpendicular to the horizontal ground, while the solid line shows a representative IP state with a sway angle θ. In this representative state, the IP experiences the gravitational force (G) and generates a ground reaction force (F_{AP}) in AP direction, which can be estimated by multiplying body mass (m) by the center of mass acceleration (aCOM). Due to the sway angle, F_{AP} includes both the corrective ground reaction force (F_{corr}) and a force resulting from the gravitational component in same direction. The right plot further explains how to calculate F_{corr}. The gravity can be decomposed into two components: the centripetal force (G_r), which equals $G * \cos\theta$, and the shear force

(G_τ), which equals $G * \sin\theta$. The effect of G_τ in the AP direction(G_{τ_AP}) can be calculated as $G_\tau * \cos\theta$, representing the gravitational component along the AP direction. Then the F_{corr} can be calculated as $F_{AP} - G_{\tau_AP}$.

Due to sensorimotor noise, the IP model will not maintain a vertical position but sways with varying ankle angle (θ). As a result, the obtained anterior-posterior ground reaction force is not equal to the corrective force (F_{corr}), but also contains a force component that is caused by gravity, as shown in Figure 2. Because our aim was the feedback effects, we isolated the corrective force by subtracting the gravitational component in the AP direction from the total ground reaction force (Figure 2).

Then, the feedback was estimated using a simple linear relationship between the preceding center of mass kinematics (deviated from the reference position) and the corrective ground reaction force:

$$F_{corr_i} = \widehat{K} * PCOM_{i-\hat{\tau}} + \widehat{B} * VCOM_{i-\hat{\tau}} + \epsilon_i \tag{2}$$

where i represents the current time, $\hat{\tau}$ is the estimated feedback delay with unit ms, F_{corr} represents the corrective ground reaction force generated by feedback control, PCOM and VCOM are the COM position and velocity accordingly. The $\widehat{K}$ and $\widehat{B}$ are the estimated position and velocity gains with unit N/m and Ns/m, respectively. ϵ represents the residual error.

Using the simulated PCOM, VCOM and calculated F_{corr}, we estimated the feedback model's control parameters ($\hat{\tau}$, $\widehat{K}$, $\widehat{B}$) and evaluated the model's goodness of fit using the coefficient of determination (R^2). Parameter estimation was performed using ordinary least square multiple regression, fitting F_{corr} to the linear model specified in equation (2) for each delay ($\hat{\tau}$). The delay at which the model achieved the maximum R^2 was regarded as the feedback delay, and the corresponding $\widehat{K}$ and $\widehat{B}$ were considered as the best estimates of the actual feedback parameters (Figure 3B). We considered F_{corr} to be sufficiently reconstructed when $R^2 \geq 0.70$. The resulting parameter estimates were averaged over the ten repetitions for subsequent analysis. In the next step, we fitted our feedback model using human experimental data.

2.2. Experimental design & data collection

15 healthy young subjects participated in this study (21± 4 yrs, 63 ± 9 kg, 1.70 ± 0.10 m, 13 females, 2 males). The experimental procedure was approved by the ethics committee of the Faculty of Behavioural and Movement Sciences, Vrije Universiteit Amsterdam. All participants received oral and written task instructions and signed written consent before the experiment.

Subjects stood quietly with feet together for 1 minute, repeating this procedure 5 times. They were instructed to face forward and maintain their arms naturally at their sides

while keeping as still as possible. Sufficient rest time was provided between trials to prevent fatigue.

Whole-body 3D kinematic data were collected at 50 sample/s using two Optotrak cameras (Northern Digital Inc., Waterloo, Ontario, Canada), with cluster markers attached to the feet, shanks, thighs, pelvis, thorax, upper arms, forearms and head. Ground reaction forces were measured with force plates embedded in the treadmill that subjects were standing on (Motek-Force-link, Amsterdam, Netherlands), and were recorded at a sampling rate of 1000 samples/s.

Raw kinematic and force data were processed using Matlab (2024a, The MathWorks, Natick, US). The raw PCOM was calculated using a 3D linked segment model developed by Kingma, deLooze, Toussaint, Klijnsma, and Bruijnen (1996). After removing the mean PCOM (the reference position of the COM in standing posture), the resulting values were used as the PCOM input for the feedback model. VCOM was calculated as the time derivative of raw PCOM. Both kinematic and force data were low-pass filtered using a second-order Butterworth filter with a cut-off frequency of 10 Hz, and the force data were down-sampled to 50 Hz. To estimate the corrective ground reaction forces (F_{corr}) from the experimental data, the gravity component was subtracted as described Figure 2.

For analysis, the data were independently analyzed for each direction. Experimental data from 6 to 50 seconds of each trial were used to fit the feedback model (equation (2)). The model fit (R^2), feedback delay ($\hat{\tau}$), feedback gains ($\widehat{K}$ and $\widehat{B}$) of all trials were estimated and averaged for further analysis. Besides, we also calculated the root mean square error (RMSE) of model residuals and the variance accounted for (VAF), to assess how well the model reconstructed F_{corr}.

The RMSE and VAF were calculated as follows:

$$RMSE = \sqrt{\frac{1}{n}\sum_{i=1}^{n}\left(F_{corr_i} - rF_{corr_i}\right)^2} \tag{3}$$

$$VAF = 1 - \frac{\sqrt{\sum_{i=1}^{n}(F_{corr_i} - rF_{corr_i})^2}}{\sqrt{\sum_{i=1}^{n} {F_{corr_i}}^2}} \tag{4}$$

Where F_{corr} is the measured corrective ground reaction force, rF_{corr} is the reconstructed F_{corr} predicted by the model, i represents current time point, the RMSE has a unit of N, while the VAF is unitless.

Because estimated feedback gains are strongly influenced by the body's inertial properties (Edwards, 2007; Peterka, 2002), normalization was performed for position gain ($\widehat{K}$) and velocity gain ($\widehat{B}$). The position gain ($\widehat{K}$) was normalized by dividing by mg/l where m is the body mass, g is the gravitational acceleration, l is the height of COM (note that this is actually a combination of two operations: first, converting the linear position gain into an angular one by means of multiplying by l^2, and then dividing this angular gain by the critical stiffness mgl). The normalized position gain $\widehat{K_n}$ is unitless and describes how many times greater the rotational stiffness is compared to the critical stiffness. The velocity gain $(\hat{B})$ was normalized by dividing by $I * f/l^2$, where I is the moment of inertia of the body with respect to the ankle calculated by Steiner's Law, and the f is the characteristic oscillation frequency which equals $2 * \pi * \sqrt{l/g}$. Similar to the position gain, the normalization of velocity gain was performed in two steps: first converting the linear velocity gain to angular gain ($\widehat{B_n} l^2$), by multiplying by l^2; then dividing this angular gain by the moment of inertia I and oscillation frequency f. The normalized velocity gain ($\widehat{B_n}$) is therefore unitless.

2.3. Data analysis

2.3.1. Model simulations

We performed a multiple linear regression analysis to investigate the relationship between actual and estimated feedback parameters in our model simulations after standardization (converting to z-scores by subtracting the mean and dividing by the standard deviation). Four independent regression models were constructed, with each estimated parameter (i.e., model fit ($\boldsymbol{R^2}$), estimated feedback delay ($\hat{\boldsymbol{\tau}}$), position gains ($\widehat{\boldsymbol{K}}$) and velocity gains ($\widehat{\boldsymbol{B}}$)) as the dependent variable, and all eight actual parameters (i.e., intrinsic parameters (i.e., $\boldsymbol{K_i}, \boldsymbol{B_i}$), feedback parameters (i.e., $\boldsymbol{K}, \boldsymbol{B}, \boldsymbol{\tau}$), motor noise ($\boldsymbol{N_m}$), sensory noise ($\boldsymbol{N_{s0}}$) and dead zone ($\boldsymbol{\theta_{th}}$)) served as the independent variables, the coefficient of determination was used to assess the model fit of each regression model.

2.3.2. Human experimental data

We used a paired t-test to compare model fit (R^2) and feedback parameters (i.e., $\hat{\tau}$, $\widehat{K_n}$, $\widehat{B_n}$) between ML and AP directions. Furthermore, we compared the root mean square (RMS) of PCOM, VCOM, the center of pressure (COP) and center of pressure velocity (VCOP) between directions using paired t-tests. All statistical analyses were performed in MATLAB (2024a, The MathWorks, Natick, US). Results were presented as mean values with standard deviations (mean ± SD).

3. Results

3.1. model simulation

Simulation results with default input parameters are shown in Figure 3 (note that this simulation does not contain intermittency). With default input parameters, the model displayed sway with a realistic amplitude and temporal structure. Specifically, the RMS

of the sway ranged from 0.0064 to 0.0076 rad, falling within the range (0.0014 - 0.014 rad) reported by Winter et al. (2001). In addition, the model yielded acceptable R^2 values, ranging from 0.74 to 0.79. Notably, the estimated feedback parameters showed systematic deviations from their true values: the estimated delay exhibited a positive bias, while the position gain and velocity gain showed negative biases. The coefficient of variation of the estimated values was relatively low (3% for delay, 4% for position and velocity gains), indicating a relatively consistent estimation. These results suggest that our feedback model tends to produce stable but biased estimates of feedback parameters under default conditions, and these biases may result from the contribution of intrinsic control, as determined by its default values.

For the simulation results across all valid input combinations of input parameters (Figure 4), the estimated feedback parameters varied around their actual feedback values. Estimates showed limited positive and negative biases as above. The magnitude of deviation from the actual values varied for different combinations of input parameters (i.e., input feedback and intrinsic parameters induced variation in estimates). Figure 4 illustrates that the main driver of changes in estimated parameters were the actual feedback parameters.

Multiple linear regression analysis was used to describe how the model fit and estimated parameters depended on the input parameters of the simulation model. We found that the coefficient of determination of each regression model was higher than 0.79. As Table 2 illustrates, motor noise had no significant effects on the model fit and estimated parameters. The model fit was mainly determined by the actual delay (τ) with a standardized regression coefficient of 0.66 (p<0.001), moreover, increasing feedback velocity gain and intrinsic damping decreased model fit with standardized regression coefficients smaller than -0.4. Increasing feedback position gain, intrinsic stiffness and sensory noise improved the model fit, whereas the dead zone decreased model fit.

The estimated feedback delay ($\hat{\tau}$) was mainly determined by the actual delay (τ) with a standardized regression coefficient of 0.86 (p < 0.001), moreover, increasing sensory noise caused a positive bias on the estimated delay, while increasing other parameters caused negative biases on the estimated delay. The estimated position gain ($\widehat{K}$) showed high correspondence with the actual position gain (K), with a standardized coefficient of 0.79 (p < 0.001). Notably, the estimated position gain was also influenced by intrinsic stiffness with a standardized coefficient of 0.90. Moreover, increasing actual delay and sensory noise caused positive biases on the estimated position gain, while increasing the feedback velocity gain, intrinsic damping, and implementing the dead zone caused a negative bias on the estimated position gain. The estimated velocity gain ($\hat{B}$) demonstrated a strong relationship with the actual velocity gain (B) with a standardized coefficient of 0.85 (p < 0.001). Additionally, increasing the actual feedback delay and

implementing the dead zone caused a negative bias on the estimated velocity gain, while increasing the other parameters caused a positive bias.

24% of the total number of simulations led to unrealistic sway, Table 3 shows the distribution of each parameter value within these unrealistic sway simulations. Most unrealistic simulations occurred when the feedback position gain (K) was low. Other larger delays (τ), lower feedback velocity gain (B), and small intrinsic stiffness (K_i) coincided with unrealistically large sway values. These findings illustrate, as is to be expected, that instability of the model mainly resulted from too low position feedback gain.

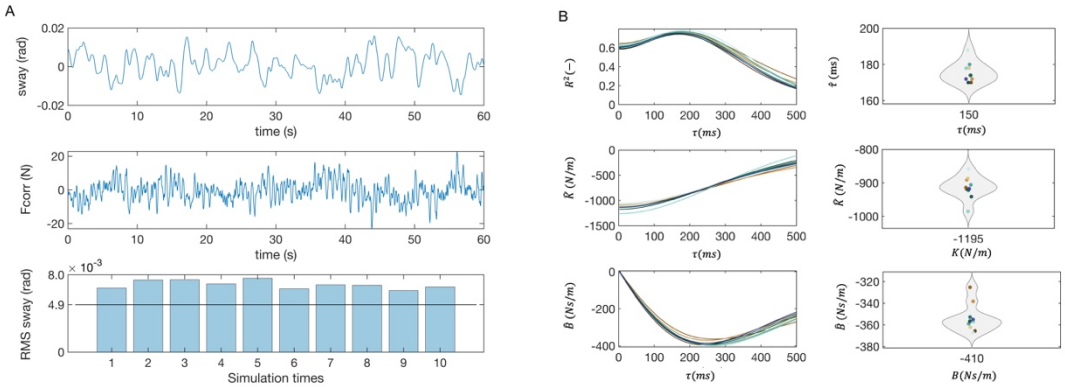

Figure 3. Model simulation results with default input parameters. Figure 3A shows the simulation results for IP sway (top panel) and the corresponding corrective ground reaction force (middle panel) from one typical simulation with default input parameters. The bottom panel shows the root mean square (RMS) of sway for 10 repeated simulations. The black line in RMS sway indicate the mean RMS sway in human upright standing (Winter et al., 2001). Figure 3B shows the feedback results obtained from the 10 simulations with default input parameters. Left panels show, as a function of the delay, the model fit (top panel), position gain (middle panel) and velocity gain (bottom panel), with different colors representing the 10 different simulations. The right side shows the parameters obtained for the delay yielding the best model fit, including estimated delay (top panel), position gain (middle panel) and velocity gain (bottom panel) as a function of the corresponding simulation input parameters. In the right side of Figure 3B, horizontal jitter was added for visualization because all data points within each violin plot share the same x-value. Note that in the middle and bottom panels, the x-axes values are converted from their input parameters by dividing by l^2, changing the original rotational stiffness and damping to linear values for direct comparison with the estimated parameters on the y-axes.

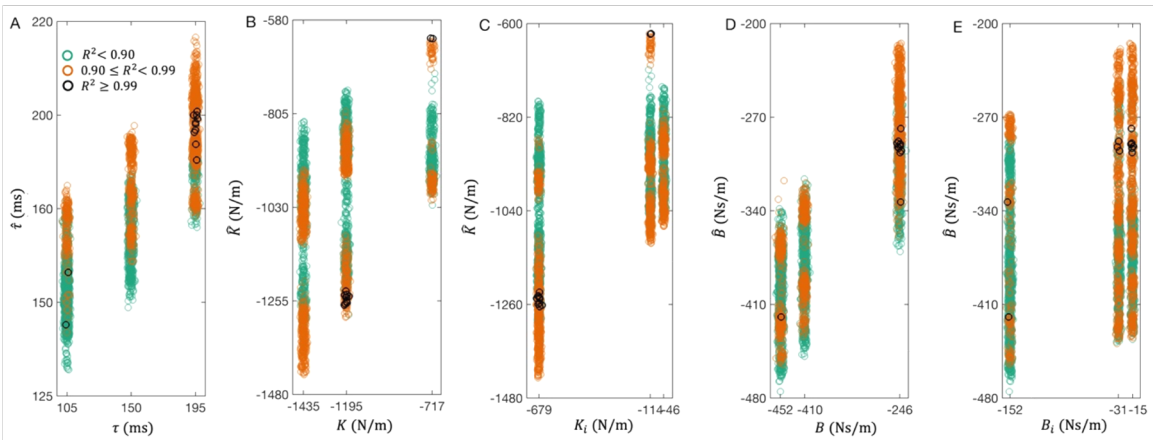

Figure 4. Estimated feedback control parameters from an inverted pendulum model with parameters varied according to Table 1. Figure 4. A-E illustrate the relationships between estimated feedback delay ($\hat{\tau}$) and actual delay (τ), the estimated position gain ($\widehat{K}$) and actual position gain (K), the estimated position gain ($\widehat{K}$) and intrinsic stiffness (K_i), the estimated velocity gain ($\hat{B}$) and actual velocity gain (B), the estimated velocity gain ($\hat{B}$) and intrinsic damping (B_i), respectively. Different colors represent parameters with different model fit, as shown in the legend. Note that in panel B, C, D, and E, the x-axes values are converted by dividing by l^2, changing the original rotational stiffness and damping to linear values for direct comparison with the estimated parameters on the y-axes.

Table 2. Standardized regression coefficients. The dependent variables are shown in the first column, with R^2, $\hat{\tau}$, $\widehat{K}$ and $\hat{B}$ being the model fit, estimated feedback delay, position and velocity gains. The independent variables are listed in the first row, with τ, K, B being the actual feedback delay, position and velocity gains, K_i, B_i the intrinsic stiffness and damping, N_m the motor noise, N_{s0} the sensory noise, θ_d the dead zone. The numbers within the table represent standardized regression coefficients, indicate one unit change in parameters of the simulation model will lead to how much change of the model fit and estimated feedback parameters. The asterisks indicating levels of significance, where * indicates $p < 0.05$ and ** indicates $p<0.001$.

	τ	K	B	K_i	B_i	N_m	N_{s0}	θ_d
R^2	0.66**	0.21**	-0.45**	0.05**	-0.40**	<0.001	0.10**	-0.15**
$\hat{\tau}$	0.86**	-0.02**	-0.26**	-0.27**	-0.37**	-0.001	0.03*	-0.03**
$\widehat{K}$	0.15**	0.79**	-0.04**	0.90**	-0.17**	0.001	0.13**	-0.14**
$\hat{B}$	-0.05*	0.10**	0.85**	0.43**	0.30**	0.002	0.07**	-0.07**

Table 3. Percentage of unrealistic sway simulations for each parameter value. 24% of the total number of simulations led to unrealistic sway. This table displays, for each parameter considered separately the percentage of the unrealistic simulation. (τ: feedback delay, K: feedback position gain, B: feedback velocity gain, K_i: intrinsic stiffness, B_i: intrinsic damping, N_m: motor noise, N_{so}: sensory noise, θ_d: dead zone).

Parameters	Values	Percentage
τ (ms)	105	29.3%
	150	29.6%
	195	41.1%
K (Nm/deg)	-581	89.0%
	-968	0.7%
	-1162	10.3%
B (Nms/deg)	-199	41.9%
	-332	29.4%
	-336	28.7%
K_i (Nm/deg)	-37	49.9%
	-92	46.0%
	-550	4.1%
B_i (Nms/deg)	-12	36.0%

	-25	35.6%
	-123	28.4%
N_m (Nm)	0.1	33.3%
	0.2	33.6%
	0.4	33.1%
N_{so} (Nm/deg)	0.0026	33.3%
	0.0052	33.3%
	0.0063	33.4%
θ_d (deg)	0	49.2%
	0.004	50.8%

3.2 Human experimental data

Figure 5A shows a typical example of the raw PCOM (top panel), VCOM (middle panel), and both raw and reconstructed corrective force (F_{corr}, bottom panel), Figure 5B shows the feedback results, including model fit (top panel); normalized position gains (middle panel); and normalized velocity gains (bottom panel) in both ML (left side) and AP (right side) directions.

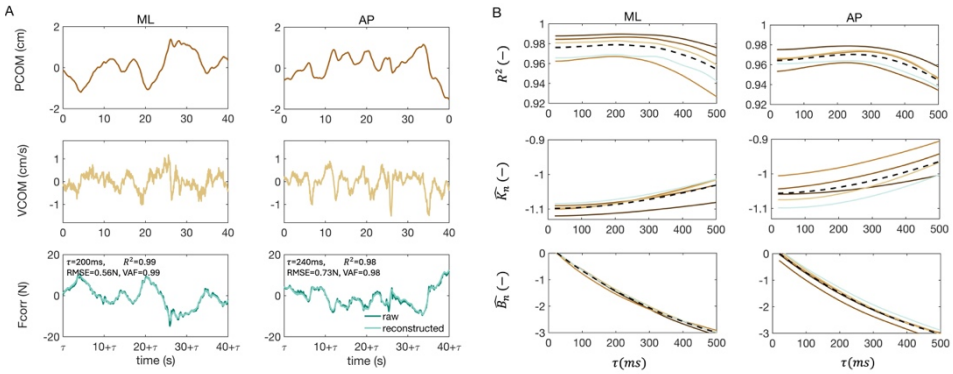

Figure 5. Time series data of model input and feedback results of one typical subject. Figure 5A shows the COM position (top panel), COM velocity (middle panel) and raw as well as reconstructed F_{corr} (bottom panel) in both ML (left side) and AP (right side) directions, respectively. Figure 5B shows the corresponding feedback results, including model fit (top panel), position gain (middle panel) and velocity gain (bottom panel), as a function of the delay. Solid colored lines represent the 5 different trials, and the bold dashed black line represents their average.

Table 4. Model fit parameters of human experimental data (mean±SD) in both ML and AP directions.

	ML	AP
R^2	0.96±0.02	0.96±0.01
RMSE (N)	0.74±0.16	0.76±0.22
VAF	0.96±0.02	0.96±0.01

F_{corr} could be effectively reconstructed from delayed PCOM and VCOM data in both ML and AP directions, with mean R^2 and VAF exceeding 0.9, and the RMSE values

below 1N. No differences in model fit were observed between directions (t (14) =-0.92, *p*>0.05, Figure 6A).

The estimated feedback delay in ML was significantly smaller than in the AP direction (*t (14)* =-4.26, *p*<0.001, Figure 6B).

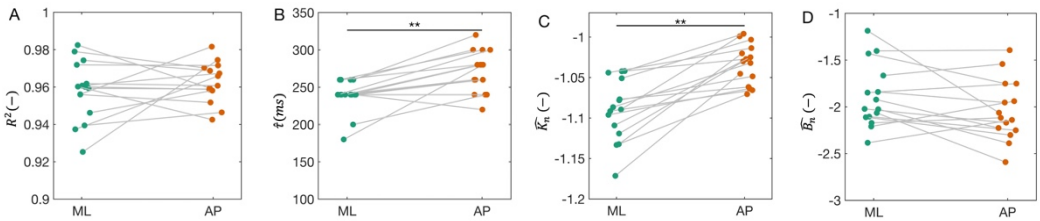

Figure 6. Feedback results of all subjects. Fit of the model (panel A) and corresponding feedback parameters: delay (panel B), normalized position gain (panel C), and normalized velocity gain (panel D). Significant differences are marked with asterisks (**: p < 0.001, *: p < 0.05).

The position gains were significantly larger in ML than in AP (*t (14)* =-6.29, *p*<0.001), with all position gains exceeding but remaining close to critical stiffness (i.e. $\widehat{K_n}$ < -1, Figure 6C).

The velocity gains were all below -1 and velocity gains were smaller in ML than in AP, while these differences were not statistically significant between directions. (*t (14) =1.85, p>0.05*; see Figure 6D).

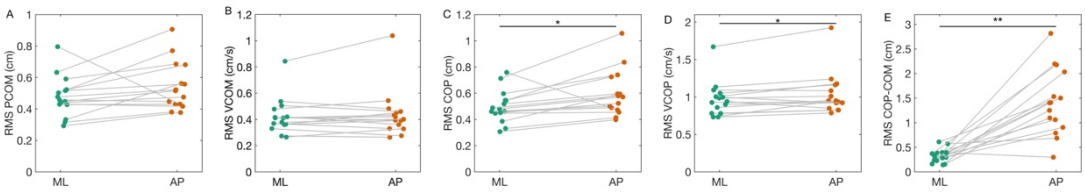

Figure 7. Root mean square (RMS) of body sway variables. RMS of center of mass position (panel A), center of mass velocity (panel B), center of pressure position (panel C), velocity of center of pressure (VCOP) (panel D), deviation between COP and COM (panel E). Significant differences are marked with asterisks (**: p < 0.001, *: p < 0.05).

There were no significant differences in the RMS values of PCOM and VCOM between directions, while the RMS values of COP, VCOP and COP-COM were significantly larger in AP than in ML.

4. Discussion

We proposed a simple linear regression model to estimate the feedback control in human standing without applying perturbations and without measurements of physiological signals, assuming that human upright stabilization can be represented by

the relationship between corrective ground reaction forces and delayed center of mass state. Both our simulation and experimental results validated this model, demonstrating that valuable information of feedback control can be efficiently estimated using this approach.

While previous research has used various models to explore feedback control involved in standing stability (Afschrift et al., 2021; De Groote et al., 2017; Morasso, 2022; Peterka, 2002; Vette, Masani, Nakazawa, & Popovic, 2010), to the best of our knowledge, this is the first study that estimated the feedback parameters in control of standing without perturbations and physiological measurements.

4.1. Model validity tested in simulation

van der Kooij et al. (2005) have argued that feedback gains cannot be identified without applying perturbations. Indeed, our model estimates the lumped contribution of all stabilizing mechanisms and parameters are to some extent biased if interpreted as reflecting feedback properties only. Specifically, our simulations showed that increased intrinsic stiffness introduces a negative bias on the estimated feedback delay and a positive bias on the estimated gains. In contrast, Le Mouel and Brette (2019) reported that increased intrinsic stiffness should be accompanied by longer neural delays and decreased feedback gains in order for a system to remain stable. This discrepancy does not represent a true contradiction, but is due to the fact that we cannot separate the intrinsic parameters and feedback control in this study. Nevertheless, the correlation between the estimated and actual feedback parameters and the dominant role of feedback control supports the use of our model to characterize human feedback control. Thus, the aforementioned limitation can be overcome if feedback gains are sufficiently large compared to intrinsic properties and feedback dominates the system's behavior. We believe that when the intrinsic parameters are relatively small compared to the feedback gains, as literature indicates (Peterka, 2002), their impact is negligible. Under such conditions, the feedback gains obtained by our model are still informative regarding the feedback mechanism.

Our model effectively reconstructed corrective ground reaction forces using center of mass position and velocity information (R^2: 0.77~0.99). Linear regression analysis showed that the estimated control parameters were closely related to the actual feedback parameters with standardized regression coefficients ranging from 0.79 to 0.86 under widely changing input parameters. This validates the model's ability to estimate feedback control in human standing, especially when the feedback plays the dominate role, despite variations of intrinsic properties, sensorimotor noise and the presence of intermittent control.

It is important to note that changes in the intrinsic parameters caused biases in estimated feedback gains, which must be considered when interpreting these

estimates in terms of feedback control exclusively. Moreover, this insight not only explains the origin of estimation biases, but also provides a basis for understanding the variability observed in human experimental data, where differences in intrinsic and feedback properties may contribute to individual or group-level differences. We do note that the intrinsic parameters were varied over a substantially wider range than the feedback parameters. Therefore, our simulation results represent a worst-case scenario.

To further validate our findings, we performed a reverse test using feedback parameters, estimated from human experimental data presented here (for the anterior-posterior direction), to drive 10 repeated simulations. We modified the model with averaged human parameters: body mass of 63kg, body height of 1.70m, feedback delay of 271ms, position gain of 744 N/m, and velocity gain of 248 Ns/m. While maintaining other parameters at their default values, we used the minimum sensorimotor noise level from our previous simulations. This approach yielded simulation results similar to those obtained from human experimental data, as detailed in Table 5 and illustrated in Figure 8. Results indicate that under more realistic conditions, our feedback model can yield reliable estimated feedback parameters, with small deviations which might be due to the intrinsic parameters and input noise.

Table 5. Model input (mean value obtained from human experimental data) and corresponding simulation results with these parameters.

	R^2	τ	$K/\hat{K}$	$B/\hat{B}$
Model input	0.96	271	-744	-248
Simulation	0.96±0.01	250±11	-769±29	-257±9

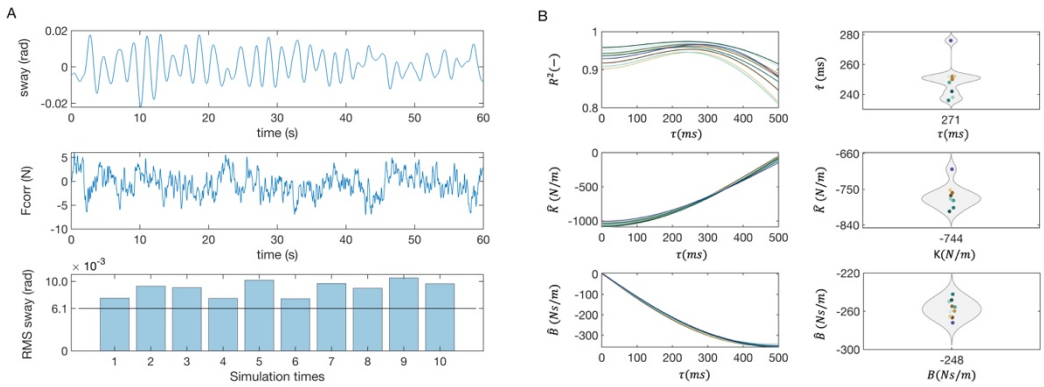

Figure 8. Model simulation results with control parameters obtained from human experimental data. Figure 8A shows the simulation results for IP sway (top panel) and the corresponding corrective ground reaction force (middle panel) from one typical simulation. The bottom panel shows the root mean square (RMS) of sway for 10 repeated simulations. The black line in RMS sway indicates the mean RMS sway in AP direction obtained from our human experimental data. Figure 8B shows the feedback results obtained from 10 simulations with parameters obtained from human results. Left panels show, as a function of the delay, the model fit (top panel), position gain (middle panel) and velocity gain (bottom panel), with different colors representing the 10 different simulations. In the right side of Figure 8B,

horizontal jitter was added for visualization because all data points within each violin plot share the same x-value.

4.2. Modeling feedback with human data

The good model fit (R^2> 0.92, VAF > 0.85) across all subjects in both AP and ML directions validates our model's capacity to accurately capture human upright stabilization mechanics and demonstrates its effectiveness in estimating feedback control parameters.

The estimated feedback delay across all subjects ranged from 180 ms to 320 ms, which is slightly larger than 100~150ms reported by some studies which usually refers to the cumulative time from stimulus to muscle activation. However, the feedback delay in our study refers to the effective delay, which includes not only the neural transmission and center nervous system decision-making delays but also the electromechanical delay between muscle excitation and force production. This estimate aligns well with the findings of Sinkjaer, Toft, Andreassen, and Hornemann (1988), reporting a peak reflex contribution timing window of 150~300 ms after the onset of stretch, as well as with Masani, Vette, Kawashima, and Popovic (2008), who reported an effective delay of 200~380 ms during quiet standing. Together, these findings support the physiological plausibility of our feedback control model.

However, one may notice that the relationship between model fit (R^2) and delay in human experimental data is quite flat (Figure 5B), which leads to uncertainty in choosing the optimal delay, and may bias the estimation of feedback gains. To assess the robustness of estimated feedback gains, we examined variations of feedback gains resulting from ±20ms changes in the delay and found that the normalized gains remained relatively unchanged (variations < 0.01 for position gains and <0.1 for velocity gains), indicating that the observed flat relationship between model fit and delay will not cause large effect on our main results.

Our analysis revealed significantly shorter feedback delays in ML compared to AP direction, along with higher position gains in ML than in AP. Based on our simulation results, these differences could be attributed to higher intrinsic stiffness in the ML direction which might be generated by the structural differences, as intrinsic stiffness can negatively bias delay estimates while positively bias position gain estimates. In the human experimental data, while no significant difference was observed in COM amplitude between directions, both COP related variables were significantly larger in AP than in ML (Figure 7). This further support the greater intrinsic stiffness in ML compared to AP.

A key finding from our study is that position gains were only slightly but consistently higher than critical stiffness in both directions, suggesting an efficient control strategy that minimizes muscle co-contraction and energy expenditure (Koelewijn & Van Den

Bogert, 2022) while maintaining stability during quiet standing. Our results suggest that healthy young adults operate slightly above-critical stability control during normal standing, which would require rapid gain adjustments to efficiently handle unexpected external perturbations while maintaining energy efficiency.

4.3. Limitations

In the model simulation, we didn't apply any external perturbation which might be the reason why we our estimated feedback parameters differ from actual feedback values. In human experimental data, we used the mean value of COM during the trial as the reference position, while the real-time COM reference may change due to rambling (Zatsiorsky & Duarte, 2000). However, if present, rambling would lead to a lower model fit as a static reference point is assumed in the model. Given the high goodness of fit, this appears not to have affected our results, possibly given the limited trial duration. Besides, the calculation of corrective ground reaction forces depends on the assumption that body can be modeled as an inverted pendulum. Obviously, this model is too simple to represent all body sway characteristics, thus this inevitably leads to some calculation errors. This limitation can be more critical in scenarios where the COM trajectory does not follow the ankle-centered circular-arch implied by the inverted pendulum model. Also, we noticed that the force plates had limited precision which could introduce noise into the force measurement. However, our model input, the F_{corr}, incorporates gravity correction and shows relatively high standard deviation, suggesting a reasonable signal-to-noise ratio. Both our experimental and simulation results support the model's validity under this condition. Moreover, our approach introduces uncertainty in the estimated feedback gains through two mechanisms. First, the relatively flat curvature in human data between model fit and delay causes uncertainty in the estimated delay which affected estimates of the feedback gains, even though this effect was quite small. Second, the lumped model used also led to errors in the estimated feedback gains, which after all reflect the lumped effect of all stabilizing mechanisms. Future studies incorporating perturbations might be helpful to estimate the extend of this error and improve the accuracy of the feedback estimation. Lastly, we did not perform any physiological measurements, making it impossible to directly relate our results to neuromuscular activity.

5. Conclusion

Our simple linear regression model provides a valuable framework for characterizing feedback control in human standing without instrumentation to induce perturbations and perform physiological measurement. While it works well in normal conditions, the validity of feedback estimates may be reduced in situations with increased intrinsic control, such as high co-contraction levels. Therefore, the validity needs to be investigated in groups with conditions that may affect movement control (e.g. old people, stability -challenging conditions). Importantly, the observation that feedback

position gain was only slightly above critical stiffness indicates efficient control, ensuring stability, while minimizing unnecessary muscle activation.

Funding

Yang Geng was funded by China Scholarship Council (No.202309370005).

CRediT authorship contribution statement

Yang Geng: Writing – original draft, Investigation, Formal analysis, Software, Conceptualization. **Sjoerd M. Bruijn:** Writing – review & editing, Methodology, Software, Conceptualization, Project administration, Supervision. **Jaap H. van Dieën:** Writing – review & editing, Methodology, Software, Conceptualization, Supervision.

Declaration of competing interest

The authors report there are no competing interests to declare.

Data availability

All data from subjects that agreed to share deidentified data and code are available at: https://zenodo.org/records/17349942.

Acknowledgements

The authors would like to thank all the subjects for their participation in the experiment and their colleagues for the help during the experiments.

References

Afschrift, M., De Groote, F., & Jonkers, I. (2021). Similar sensorimotor transformations control balance during standing and walking. *PLoS Comput Biol, 17*(6), e1008369. doi:10.1371/journal.pcbi.1008369

Amiri, P., Mohebbi, A., & Kearney, R. (2019). Experimental Methods to Study Human Postural Control. *J Vis Exp*(151). doi:10.3791/60078

Asai, Y., Tasaka, Y., Nomura, K., Nomura, T., Casadio, M., & Morasso, P. (2009). A model of postural control in quiet standing: robust compensation of delay-induced instability using intermittent activation of feedback control. *PLoS One, 4*(7), e6169. doi:10.1371/journal.pone.0006169

Casadio, M., Morasso, P. G., & Sanguineti, V. (2005). Direct measurement of ankle stiffness during quiet standing: implications for control modelling and clinical application. *Gait Posture, 21*(4), 410-424. doi:10.1016/j.gaitpost.2004.05.005

Creath, R., Kiemel, T., Horak, F., Peterka, R., & Jeka, J. (2005). A unified view of quiet and

perturbed stance: simultaneous co-existing excitable modes. *Neurosci Lett, 377*(2), 75-80. doi:10.1016/j.neulet.2004.11.071

De Groote, F., Allen, J. L., & Ting, L. H. (2017). Contribution of muscle short-range stiffness to initial changes in joint kinetics and kinematics during perturbations to standing balance: A simulation study. *J Biomech, 55*, 71-77. doi:10.1016/j.jbiomech.2017.02.008

de Vlugt, E., van Eesbeek, S., Baines, P., Hilte, J., Meskers, C. G., & de Groot, J. H. (2011). Short range stiffness elastic limit depends on joint velocity. *J Biomech, 44*(11), 2106-2112. doi:10.1016/j.jbiomech.2011.05.022

Edwards, W. T. (2007). Effect of joint stiffness on standing stability. *Gait Posture, 25*(3), 432-439. doi:10.1016/j.gaitpost.2006.05.009

Gage, W. H., Winter, D. A., Frank, J. S., & Adkin, A. L. (2004). Kinematic and kinetic validity of the inverted pendulum model in quiet standing. *Gait Posture, 19*(2), 124-132. doi:10.1016/S0966-6362(03)00037-7

Gatev, P., Thomas, S., Kepple, T., & Hallett, M. (1999). Feedforward ankle strategy of balance during quiet stance in adults. *J Physiol, 514 (Pt 3)*(Pt 3), 915-928. doi:10.1111/j.1469-7793.1999.915ad.x

Goodworth, A. D., & Peterka, R. J. (2010). Influence of stance width on frontal plane postural dynamics and coordination in human balance control. *Journal of Neurophysiology, 104*(2), 1103-1118. doi:10.1152/jn.00916.2009

Kelton, I. W., & Wright, R. D. (1949). The Mechanism of Easy Standing by Man. *Australian Journal of Experimental Biology and Medical Science, 27*(5), 505-515. doi:DOI 10.1038/icb.1949.49

Kingma, I., deLooze, M. P., Toussaint, H. M., Klijnsma, H. G., & Bruijnen, T. B. M. (1996). Validation of a full body 3-D dynamic linked segment model. *Human Movement Science, 15*(6), 833-860. doi:Doi 10.1016/S0167-9457(96)00034-6

Koelewijn, A. D., & Van Den Bogert, A. J. (2022). Antagonistic co-contraction can minimize muscular effort in systems with uncertainty. *PeerJ, 10*, e13085. doi:10.7717/peerj.13085

Latash, M. L., & Zatsiorsky, V. M. (1993). Joint Stiffness - Myth or Reality. *Human Movement Science, 12*(6), 653-692. doi:Doi 10.1016/0167-9457(93)90010-M

Le Mouel, C., & Brette, R. (2019). Anticipatory coadaptation of ankle stiffness and sensorimotor gain for standing balance. *PLoS Comput Biol, 15*(11), e1007463. doi:10.1371/journal.pcbi.1007463

Loram, I. D., Gollee, H., van de Kamp, C., & Gawthrop, P. J. (2022). Is Intermittent Control the Source of the Non-Linear Oscillatory Component (0.2-2Hz) in Human Balance Control? *IEEE Trans Biomed Eng, 69*(12), 3623-3634. doi:10.1109/TBME.2022.3174927

Loram, I. D., & Lakie, M. (2002). Direct measurement of human ankle stiffness during quiet standing: the intrinsic mechanical stiffness is insufficient for stability. *J Physiol, 545*(3), 1041-1053. doi:10.1113/jphysiol.2002.025049

Masani, K., Vette, A. H., Kawashima, N., & Popovic, M. R. (2008). Neuromusculoskeletal torque-generation process has a large destabilizing effect on the control mechanism of quiet standing. *Journal of Neurophysiology, 100*(3), 1465-1475. doi:10.1152/jn.00801.2007

Mello, E. M., Magalhaes, F. H., & Kohn, A. F. (2013). Larger plantar flexion torque variability

implies less stable balance in the young: an association affected by knee position. *Hum Mov Sci, 32*(6), 1310-1324. doi:10.1016/j.humov.2013.05.004

Milton, J., Townsend, J. L., King, M. A., & Ohira, T. (2009). Balancing with positive feedback: the case for discontinuous control. *Philos Trans A Math Phys Eng Sci, 367*(1891), 1181-1193. doi:10.1098/rsta.2008.0257

Morasso, P. (2022). Integrating ankle and hip strategies for the stabilization of upright standing: An intermittent control model. *Front Comput Neurosci, 16*, 956932. doi:10.3389/fncom.2022.956932

Pai, Y. C., & Patton, J. (1997). Center of mass velocity-position predictions for balance control. *J Biomech, 30*(4), 347-354. doi:10.1016/s0021-9290(96)00165-0

Peterka, R. J. (2002). Sensorimotor integration in human postural control. *Journal of Neurophysiology, 88*(3), 1097-1118. Retrieved from https://www.ncbi.nlm.nih.gov/pubmed/12205132 https://journals.physiology.org/doi/pdf/10.1152/jn.2002.88.3.1097

Rack, P. M., & Westbury, D. R. (1974). The short range stiffness of active mammalian muscle and its effect on mechanical properties. *J Physiol, 240*(2), 331-350. doi:10.1113/jphysiol.1974.sp010613

Ribeiro, G. A., Knop, L. N., & Rastgaar, M. (2020). Multi-Directional Ankle Impedance During Standing Postures. *IEEE Trans Neural Syst Rehabil Eng, 28*(10), 2224-2235. doi:10.1109/TNSRE.2020.3018650

Safavynia, S. A., & Ting, L. H. (2013). Long-latency muscle activity reflects continuous, delayed sensorimotor feedback of task-level and not joint-level error. *Journal of Neurophysiology, 110*(6), 1278-1290. doi:10.1152/jn.00609.2012

Sakanaka, T. E., Gill, J., Lakie, M. D., & Reynolds, R. F. (2018). Intrinsic ankle stiffness during standing increases with ankle torque and passive stretch of the Achilles tendon. *PLoS One, 13*(3), e0193850. doi:10.1371/journal.pone.0193850

Shi, F., Rymer, W. Z., & Son, J. (2023). Ankle Joint Angle Influences Relative Torque Fluctuation during Isometric Plantar Flexion. *Bioengineering (Basel), 10*(3). doi:10.3390/bioengineering10030373

Shiozawa, K., Lee, J., Russo, M., Sternad, D., & Hogan, N. (2021). Frequency-dependent force direction elucidates neural control of balance. *J Neuroeng Rehabil, 18*(1), 145. doi:10.1186/s12984-021-00907-2

Sinkjaer, T., Toft, E., Andreassen, S., & Hornemann, B. C. (1988). Muscle stiffness in human ankle dorsiflexors: intrinsic and reflex components. *Journal of Neurophysiology, 60*(3), 1110-1121. doi:10.1152/jn.1988.60.3.1110

Sugimoto-Dimitrova, R., Shiozawa, K., Gruben, K. G., & Hogan, N. (2024). Frequency-domain patterns in foot-force line-of-action: an emergent property of standing balance control. *Journal of Neurophysiology, 132*(5), 1445-1456. doi:10.1152/jn.00084.2024

van der Kooij, H., van Asseldonk, E., & van der Helm, F. C. (2005). Comparison of different methods to identify and quantify balance control. *J Neurosci Methods, 145*(1-2), 175-203. doi:10.1016/j.jneumeth.2005.01.003

van Dieen, J. H., Bruijn, S. M., & Afschrift, M. (2024). Assessment of stabilizing feedback control of

walking: A tutorial. *J Electromyogr Kinesiol, 78*, 102915. doi:10.1016/j.jelekin.2024.102915

Vette, A. H., Masani, K., Nakazawa, K., & Popovic, M. R. (2010). Neural-mechanical feedback control scheme generates physiological ankle torque fluctuation during quiet stance. *IEEE Trans Neural Syst Rehabil Eng, 18*(1), 86-95. doi:10.1109/TNSRE.2009.2037891

Winter, D. A., Patla, A. E., Prince, F., Ishac, M., & Gielo-Perczak, K. (1998). Stiffness control of balance in quiet standing. *Journal of Neurophysiology, 80*(3), 1211-1221. doi:10.1152/jn.1998.80.3.1211

Winter, D. A., Patla, A. E., Rietdyk, S., & Ishac, M. G. (2001). Ankle muscle stiffness in the control of balance during quiet standing. *Journal of Neurophysiology, 85*(6), 2630-2633. doi:10.1152/jn.2001.85.6.2630

Zatsiorsky, V. M., & Duarte, M. (2000). Rambling and trembling in quiet standing. *Motor Control, 4*(2), 185-200. doi:10.1123/mcj.4.2.185